11-2007

Impacts of large-scale oscillations on pan-Arctic terrestrial net primary production

Ke Zhang
The University of Montana

John S. Kimball
University of Montana - Missoula

K. C. McDonald

John Cassano

Steven W. Running
University of Montana - Missoula

Recommended Citation

Zhang, K., J. S. Kimball, K. C. McDonald, J. J. Cassano, and S. W. Running (2007), Impacts of large-scale oscillations on pan-Arctic terrestrial net primary production, Geophys. Res. Lett., 34, L21403, doi:10.1029/2007GL031605

GEOPHYSICAL RESEARCH LETTERS, VOL. 34, L21403, doi:10.1029/2007GL031605, 2007

Impacts of large-scale oscillations on pan-Arctic terrestrial net primary production

Ke Zhang,[1,2] John S. Kimball,[1,2] Kyle C. McDonald,[3] John J. Cassano,[4] and Steven W. Running[2]

Received 6 August 2007; revised 28 September 2007; accepted 8 October 2007; published 7 November 2007.

[1] Analyses of regional climate oscillations and satellite remote sensing derived net primary production (NPP) and growing season dynamics for the pan-Arctic region indicate that the oscillations influence NPP by regulating seasonal patterns of low temperature and moisture constraints to photosynthesis. Early-spring (Feb–Apr) patterns of the Arctic Oscillation (AO) are proportional to growing season onset ($r = -0.653$; $P = 0.001$), while growing season patterns of the Pacific Decadal Oscillation (PDO) are proportional to plant-available moisture constraints to NPP (I_m) ($r = -0.471$; $P = 0.023$). Relatively strong, negative PDO phases from 1988–1991 and 1998–2002 coincided with prolonged regional droughts indicated by a standardized moisture stress index. These severe droughts resulted in widespread reductions in NPP, especially for relatively drought prone boreal forest and grassland/cropland ecosystems. The influence of AO and PDO patterns on northern vegetation productivity appears to be decreasing and increasing, respectively, as low temperature constraints to plant growth relax and NPP becomes increasingly limited by available water supply under a warming climate. **Citation:** Zhang, K., J. S. Kimball, K. C. McDonald, J. J. Cassano, and S. W. Running (2007), Impacts of large-scale oscillations on pan-Arctic terrestrial net primary production, *Geophys. Res. Lett.*, *34*, L21403, doi:10.1029/2007GL031605.

1. Introduction

[2] Low temperatures, plant-available water stress and limited solar irradiance are the primary environmental constraints on vegetation net primary production (NPP) in the pan-Arctic region [*Churkina and Running*, 1998; *Jolly et al.*, 2005]. The low temperature constraint to vegetation growth is relaxing with global warming [*Trenberth et al.*, 2007; *Hassol et al.*, 2004], resulting in earlier and longer growing seasons [*McDonald et al.*, 2004] and generally increased vegetation greenness and productivity [*Lucht et al.*, 2002; *Kimball et al.*, 2006; *Zhang et al.*, 2007]. However, warmer temperatures also coincide with increases in vegetation moisture stress and recent, widespread drought within the pan-Arctic region [*Angert et al.*, 2005; *Schindler and Donahue*, 2006], resulting in declines in vegetation greenness and production, especially for boreal forests [*Goetz et al.*, 2005].

[3] Large-scale atmospheric [*Wallace and Thompson*, 2002] and ocean [*Siedler et al.*, 2001] circulation patterns have significant impacts on regional and global climate variability, and a growing body of evidence indicates that ocean-atmosphere induced climate oscillations also influence terrestrial NPP [*Lotsch et al.*, 2005]. The Arctic Oscillation (AO) [*Thompson and Wallace*, 1998] and the Pacific Decadal Oscillation (PDO) [*Mantua et al.*, 1997] are the major large-scale oscillations influencing pan-Arctic regional climate. The AO is defined as the leading principal component of sea level pressure (SLP) variability in the Northern Hemisphere and is a robust surface manifestation of the strength of the polar vortex [*Thompson and Wallace*, 1998]. The AO is reported to influence winter Eurasian snow cover [*Gong et al.*, 2003] and Hudson Bay river discharge [*Déry and Wood*, 2004]. The PDO is the leading principal component of North Pacific sea surface temperature (SST) variability [*Mantua et al.*, 1997] and has been correlated with North American precipitation and stream flow [*Dettinger et al.*, 1998], and northeast Asia surface air temperature fluctuations [*Minobe*, 2000].

[4] We hypothesized that the AO and PDO influence pan-Arctic terrestrial production by regulating the timing of annual growing season onset and the supply of plant-available moisture. We examined spatio-temporal correlations between early-spring (Feb–Apr) patterns of the two oscillations and the timing of growing season onset. We also examined the role of the two oscillations in explaining temporal anomalies in growing season vapor pressure deficit (VPD) derived moisture stress.

2. Data and Methods

[5] The study domain encompasses the pan-Arctic basin and Alaska including all land areas draining into the Arctic Ocean, Hudson Bay, James Bay, Hudson Strait, and the Bering Sea (Figure 1a).

2.1. PEM NPP Series and Moisture Stress Index

[6] Daily NPP series were derived from 1983–2005 on a grid cell-by-cell basis with 16 km × 16 km resolution using the MOD17A2/A3 production efficiency model (PEM) [*Running et al.*, 2000, 2004; *Heinsch et al.*, 2003] driven by satellite remote sensing based monthly leaf area index (LAI) and fraction of photosynthetically active radiation (FPAR) developed from NOAA Advanced Very High-

[1]Flathead Lake Biological Station, University of Montana, Polson, Montana, USA.
[2]Numerical Terradynamic Simulation Group, University of Montana, Missoula, Montana, USA.
[3]Jet Propulsion Laboratory, California Institute of Technology, Pasadena, California, USA.
[4]Cooperative Institute for Research in Environmental Sciences and Department of Atmospheric and Oceanic Sciences, University of Colorado, Boulder, Colorado, USA.

0094-8276/07/2007GL031605$05.00

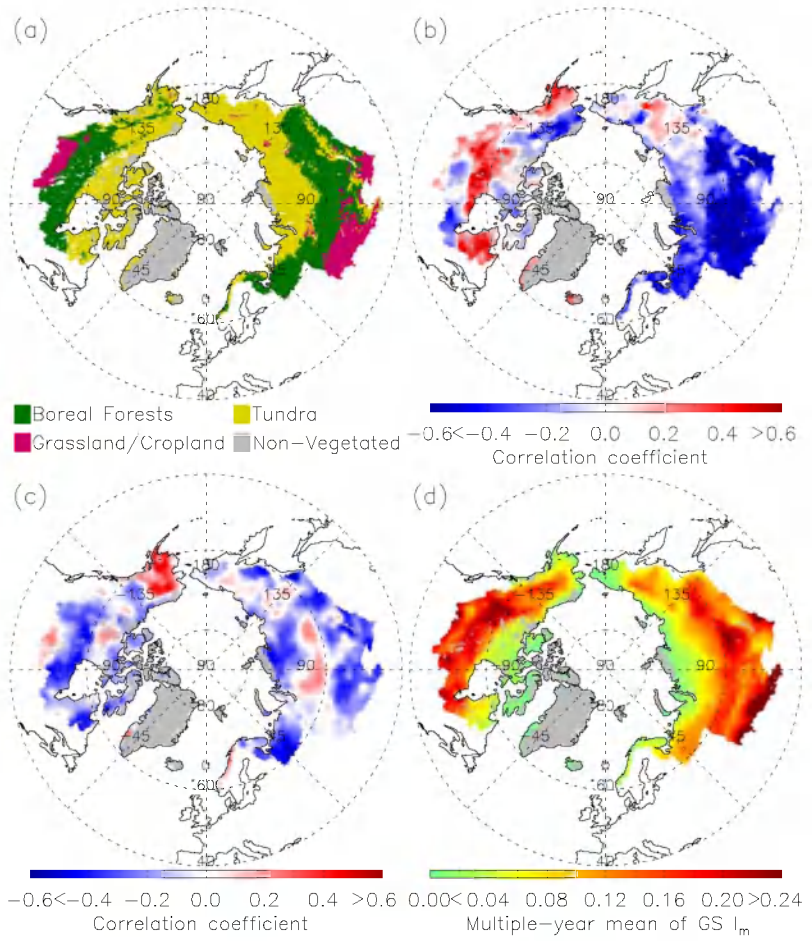

Figure 1. (a) Major biomes within the Pan-Arctic domain as defined from the NASA IGBP-MODIS global land cover classification. Correlation maps (b) between AO_{spr} and the timing of growing season onset derived from PEM calculations and (c) between PDO_{GS} and GS I_m. (d) The map of mean (23-year) GS I_m values for the pan-Arctic domain.

Resolution Radiometer (AVHRR) Pathfinder and NASA MODerate resolution Imaging Spectroradiometer (MODIS) records, and a gridded daily surface meteorological dataset developed from a regional correction of the NCEP/NCAR reanalysis and NASA Solar Radiation Budget daily shortwave solar radiation inputs (see the auxiliary material).[1]

[7] To quantify the moisture constraints to NPP, we defined a simple moisture stress index (I_m) based on the PEM algorithms (see the auxiliary material). The I_m parameter is dimensionless, ranging from 0 to 1 with increasing VPD constraints to NPP. We calculated a potential annual NPP rate ($NPP_{potential}$) by eliminating the VPD based moisture constraint in the PEM calculations. We then determined the proportional difference between annual NPP calculations under potential and actual conditions as a simple loss index: $\delta_{NPP\_Loss} = \frac{NPP_{potential} - NPP_{actual}}{NPP_{potential}}$. The δ_{NPP_Loss} values were then standardized using estimated means and standard deviations of the 1983–2005 time series. The standardized value of δ_{NPP_Loss} (SI_{NPP_Loss}) represents a direct measure of drought-induced NPP losses, whereas the I_m parameter describes the relative strength of the VPD defined moisture constraint on NPP calculations.

2.2. Timing of Growing Season Onset

[8] The timing (day of year) of growing season onset was derived from two different approaches, including: the seasonal onset of terrestrial NPP (T_{NPP}) derived from the PEM, and timing of the spring drawdown of atmospheric CO_2 concentrations (T_{CO_2}) from NOAA GMD arctic and sub-arctic monitoring stations (>50°N) (see the auxiliary material).

2.3. Climate Oscillations

[9] The monthly PDO indices were provided by the University of Washington (http://jisao.washington.edu/pdo/), while monthly AO indices were obtained from the US National Weather Service Climate Prediction Center.

[10] To analyze the relationship between oscillations and the timing of growing season onset in the region, we first calculated early-spring mean values of the monthly oscillation indices, and then standardized the values using the means and standard deviations. We then conducted a pixel-wise correlation analysis between the oscillation indices and T_{NPP} time series. The same procedures were applied to evaluate linkages between mean oscillation

[1] Auxiliary materials are available in the HTML. doi:10.1029/2007GL031605.

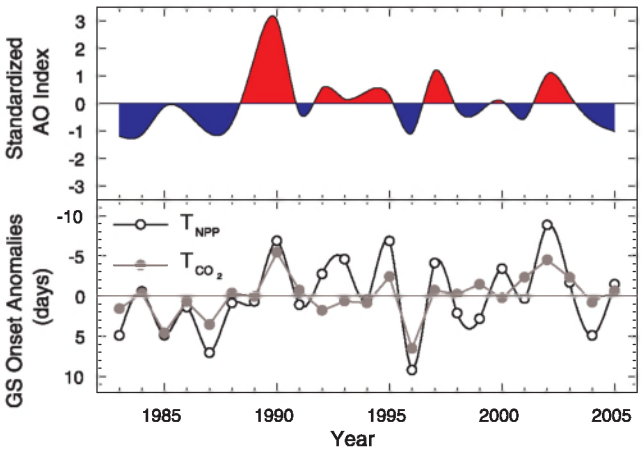

Figure 2. Temporal trajectories of the AO_{spr} and annual anomalies of regional average growing season onset derived from PEM calculations (T_{NPP}), and the seasonal pattern of atmospheric CO_2 concentrations (T_{CO_2}); negative anomalies denote earlier onset of the growing season, while positive values denote the opposite response relative to the 23-year record.

indices during the growing season, I_m and SI_{NPP_Loss}. The growing season (GS, Apr–Oct) is defined as all months in which the 1983–2005 monthly average air temperature for the pan-Arctic domain is above 0.0°C.

3. Results

[11] Only the spring AO index (AO_{spr}) showed a strong systematic correlation with T_{NPP}. The correlations between AO_{spr} and T_{NPP} were predominantly negative for the Eurasian portion of the domain, but positive for Central and Northeastern Canada (Figure 1b). This is because a positive AO_{spr} reflects stronger-than-normal pressure patterns, resulting in stronger-than-normal westerly winds across the North Atlantic Ocean in the 40°N–60°N latitude belt, warmer-than-normal conditions and earlier growing season onset over Eurasia, and colder-than-normal conditions and later growing season onset over the eastern Canadian Arctic [*Hurrell*, 1996]. The pan-Arctic regional average T_{NPP} was negatively correlated with AO_{spr} ($r = -0.653$; $P = 0.001$) (Figure 2). The relatively strong correlation ($r = 0.777$; $P < 0.001$) between T_{CO_2} and regional average T_{NPP} (Figure 2) also indicates that northern terrestrial ecosystems dominate the seasonal atmospheric CO_2 cycle at high northern latitudes and that the PEM captures the annual timing of the growing season onset. Positive AO_{spr} phases coincided with generally earlier growing season onset, while negative AO_{spr} phases are concurrent with later growing season onset.

[12] These results indicate that regional oscillations captured by the AO_{spr} influence annual NPP by affecting the timing of growing season onset. Previous studies indicate that approximately 1% of annual NPP is gained or lost for each additional day advance or delay in the annual onset of the growing season [*Kimball et al.*, 2004, 2006; *Baldocchi et al.*, 2001]. Within the pan-Arctic domain, 86.6% of the vegetated area showed a negative correlation between the timing of growing season onset and annual NPP for the 1983–2005 period, while 59.3% of this area showed a significant correlation with at least 90% confidence. A temporal advance in growing season onset promotes vegetation growth by increasing the potential annual duration of photosynthesis, but may not necessary lead to greater annual vegetation production because of other influences on NPP including plant-available moisture constraints to photosynthesis, fire and related disturbance impacts during the growing season.

[13] The spatial patterns of correlations between the growing season oscillations and GS I_m indicate that only the PDO_{GS} shows strong systematic association with GS I_m. The PDO_{GS} and GS I_m relationship (Figure 1c) is predominantly negative for Southern, Central and Northeastern Canada, and Northwestern and Southern Eurasia indicating a reduced VPD constraint to NPP for positive PDO conditions, but positive for Western and Southern Alaska. Overall, approximately 75.7% of the domain showed a negative correlation between PDO_{GS} and GS I_m for the 23-year period, 29.6% of which showed a significant correlation with at least 90% confidence. Approximately 50.7% of this area showed above-average moisture stress (i.e. greater than average moisture stress relative to the 23-year pan-Arctic regional mean) that was predominantly located in boreal forest and grassland/cropland biomes, rather than tundra (Figures 1a and 1d).

[14] The PDO_{GS} index was correlated to regional average GS I_m ($r = -0.471$; $P = 0.023$) (Figure 3), indicating that North Pacific SST patterns during the growing season

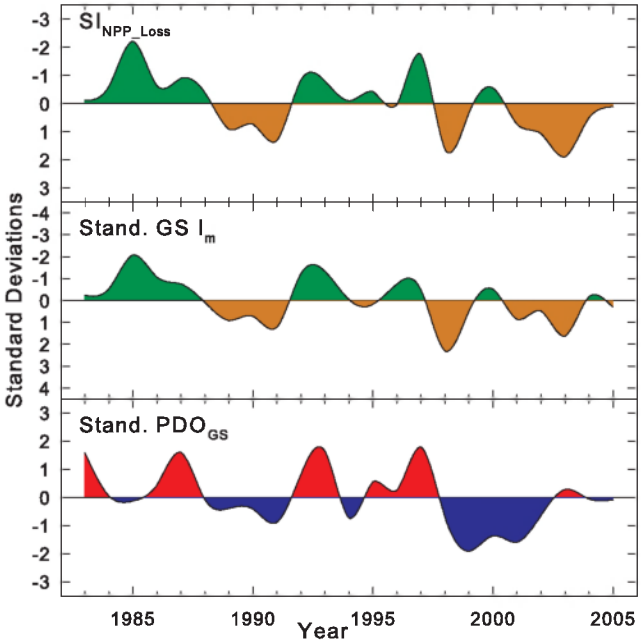

Figure 3. Time plots of SI_{NPP_Loss}, and standardized GS I_m and PDO_{GS} anomalies for the pan-Arctic domain. SI_{NPP_Loss} represents drought-induced NPP losses relative to potential conditions, where less-than-normal (green) and larger-than-normal (brown) NPP losses are standardized relative to 23-year mean conditions. Positive PDO_{GS} phases (red) generally corresponded to wetter-than-normal conditions (green), whereas negative PDO_{GS} phases (blue) were generally related to drier-than-normal conditions (brown).

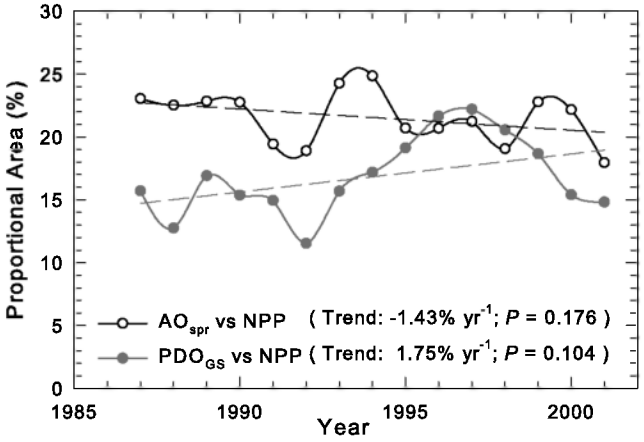

Figure 4. Time series of the proportional area of the pan-Arctic domain showing significant correlation between AO_{spr} and annual NPP and the proportional area of drought prone regions having significant correlations between PDO_{GS} and annual NPP, where the 23-year mean GS I_m exceeds regional mean conditions. The time series represents a nine-year moving correlation analysis, while dashed lines show the linear trends for the time series.

impact atmospheric moisture inputs to the pan-Arctic land mass, especially for boreal forest and grassland/cropland biomes. Positive phases of the PDO_{GS} generally correspond to wetter-than-normal conditions, while the negative PDO_{GS} phases were concurrent with drier-than-normal conditions for the region. The PDO_{GS} index was also significantly correlated with SI_{NPP_Loss} ($r = -0.485$; $P = 0.019$). The relative influence of PDO_{GS} on GS I_m also showed substantial spatial (Figure 1c) and temporal variability (Figure 3). Both GS I_m and SI_{NPP_Loss} indicated two widespread and prolonged droughts that resulted in substantial NPP declines from 1988–1991 and 1998–2003. The most recent drought resulted in particularly large NPP losses relative to the 23-year record. Drought-induced NPP losses in 1998, 2002, and 2003 were 1.63, 1.07 and 1.90 standard deviations from mean (23-year) conditions. Both of these droughts corresponded to negative PDO_{GS} phases. The most severe (1998–2003) regional drought coincided with a particularly strong negative PDO_{GS} phase. A previous study [*MacDonald and Case*, 2005] also reported that a prolonged and strongly negative PDO phase between AD 993 and 1300 is contemporaneous with a severe medieval mega-drought that is apparent in many proxy hydrologic records for the western United States and Canada. Although the PDO_{GS} didn't show strong correspondence with SI_{NPP_Loss} in 2000 and 2003, the relatively weak correlation between PDO_{GS} and SI_{NPP_Loss} within less drought prone tundra regions may be partially responsible for this. Since the oceans are the major atmospheric moisture source for the pan-Arctic land mass, the correspondence between PDO_{GS} and SI_{NPP_Loss} indicates that large-scale oscillations characterized by the PDO have a major impact on northern terrestrial NPP by regulating the supply of plant-available moisture during the growing season. However, the effect of the PDO on NPP shows strong spatial and temporal variability depending on the sign and relative strength of the PDO phase, and the potential vulnerability of vegetation to drought. The effect of PDO_{GS} on NPP appears to be larger within continental interior regions and southern margins of the boreal forest and grassland/cropland biomes where warmer air temperatures, longer potential growing seasons and a limited summer moisture supply result in larger potential moisture constraints to regional production. The recent increasing trend in GS I_m has been attributed to decreasing plant-available water supply and increasing air temperature, rather than changes in solar irradiance (Figure S1). The relative impact of the oscillations on regional productivity may also be changing as regional warming trends increase potential growing seasons and GS air temperatures.

[15] To assess temporal trends in the relations between AO_{spr} and PDO_{GS} patterns, and annual NPP, we calculated time series of the proportional areas (%) of the pan-Arctic domain showing significant correlations between annual NPP and AO_{spr}, and between annual NPP and PDO_{GS} using a nine-year moving correlation analysis (see the auxiliary material). The NPP-PDO_{GS} relationship was only assessed for drought prone areas where the 23-year mean GS I_m value exceeded pan-Arctic regional mean conditions, because the drought prone areas covered 50.4% of the total vegetated area, and PDO_{GS} generally showed insignificant ($P > 0.1$) correspondence to GS I_m for other areas. The proportional area showing a significant correlation between AO_{spr} and annual NPP decreased by 1.43% per year ($P = 0.176$) from 1983 to 2005 (Figure 4), indicating that the AO_{spr} influenced timing of growing season onset became less important to annual NPP as low-temperature constraints to photosynthesis relaxed under an observed (0.5°C per decade; $P = 0.002$) positive trend in GS air temperature for the period of record (Figure S1). Coincidently, the proportional area of drought prone regions showing significant correlations between PDO_{GS} and annual NPP increased by 1.75% per year ($P = 0.104$), indicating that the PDO_{GS} influenced supply of plant-available moisture became an increasing constraint on annual productivity with regional warming. However, the significance of these trends is limited by the relatively short duration of the satellite record.

4. Conclusions

[16] Synchronous ocean-atmosphere oscillations of the North Pacific, North Atlantic, and Arctic regions have a strong impact on the seasonal cycle and magnitude of pan-Arctic vegetation productivity and the regional uptake and sequestration of atmospheric CO_2 by vegetation biomass. These oscillations affect NPP by influencing the seasonal pattern of low temperature and moisture constraints to photosynthesis. The early-spring pattern of the AO influences the timing of growing season onset within the pan-Arctic domain, while growing season PDO patterns correspond with the supply of plant-available moisture. As potential growing seasons become longer under a warming climate, negative phases of the PDO may have increasingly widespread and negative impacts on northern terrestrial uptake and sequestration of atmospheric CO_2, as plant-available moisture becomes more limiting to NPP. The two largest observed drought-induced reductions in regional productivity occurred during the latter half of the 23-year

satellite record and coincided with particularly strong, negative PDO_{GS} phases. The influence of the springtime AO on terrestrial production is likely to decline under current warming trends as low temperature constraints to vegetation growth relax and NPP becomes increasingly constrained by the available supply of moisture during the growing season.

[17] **Acknowledgments.** This work was supported by NASA Headquarters under the NASA Earth and Space Science Fellowship Program-Grant "NNX07AN78H", NASA Earth Science Enterprise program (NNG04GJ44G), and the NSF Office of Polar Programs (3702AP15297803211). Portions of this work were performed at the Jet Propulsion Laboratory, California Institute of Technology, under contract to the National Aeronautics and Space Administration.

References

Angert, A., et al. (2005), Drier summers cancel out the CO_2 uptake enhancement induced by warmer springs, *Proc. Natl. Acad. Sci. U. S. A.*, *102*, 10,823–10,827.

Baldocchi, D., et al. (2001), FLUXNET: A new tool to study the temporal and spatial variability of ecosystem-scale carbon dioxide, water vapor, and energy flux densities, *Bull. Am. Meteorol. Soc.*, *82*, 2415–2434.

Churkina, G., and S. W. Running (1998), Contrasting climatic controls on the estimated productivity of global terrestrial biomes, *Ecosystems*, *1*, 206–215.

Déry, S. J., and E. F. Wood (2004), Teleconnection between the Arctic Oscillation and Hudson Bay river discharge, *Geophys. Res. Lett.*, *31*, L18205, doi:10.1029/2004GL020729.

Dettinger, M. D., et al. (1998), North-south precipitation patterns in western North America on interannual-to-decadal timescales, *J. Clim.*, *11*, 3095–3111.

Goetz, S. J., A. G. Bunn, G. J. Fiske, and R. A. Houghton (2005), Satellite-observed photosynthetic trends across boreal North America associated with climate and fire disturbance, *Proc. Natl. Acad. Sci. U. S. A.*, *102*, 13,521–13,525.

Gong, G., D. Entekhabi, and J. Cohen (2003), Relative impacts of Siberian and North American snow anomalies on the winter Arctic Oscillation, *Geophys. Res. Lett.*, *30*(16), 1848, doi:10.1029/2003GL017749.

Hassol, S. J., et al. (2004), *Impacts of a Warming Arctic*, 139 pp., Cambridge Univ. Press, Cambridge, U. K.

Heinsch, F. A., et al. (2003), User's guide, GPP and NPP (MOD17A2/A3) products NASA MODIS land algorithm, version 2.0, 57 pp., Univ. of Mont., Missoula.

Hurrell, J. W. (1996), Influence of variations in extratropical winter-time teleconnections on Northern Hemisphere temperature, *Geophys. Res. Lett.*, *23*, 665–668.

Jolly, W. M., R. Nemani, and S. W. Running (2005), A generalized, bioclimatic index to predict foliar phenology in response to climate, *Global Change Biol.*, *11*, 619–632.

Kimball, J. S., et al. (2004), Radar remote sensing of the spring thaw transition across a boreal landscape, *Remote Sens. Environ.*, *89*, 163–175.

Kimball, J. S., et al. (2006), Satellite remote sensing of terrestrial net primary production for the pan-Arctic basin and Alaska, *Mitigation Adaptation Strategies Global Change*, *11*, 782–804, doi:10.1007/s11027-005-9014-5.

Lotsch, A., M. A. Friedl, B. T. Anderson, and C. J. Tucker (2005), Response of terrestrial ecosystems to recent Northern Hemispheric drought, *Geophys. Res. Lett.*, *32*, L06705, doi:10.1029/2004GL022043.

Lucht, W., et al. (2002), Climatic control of the high-latitude vegetation greening trend and pinatubo effect, *Science*, *296*, 1687–1689.

MacDonald, G. M., and R. A. Case (2005), Variations in the Pacific Decadal Oscillation over the past millennium, *Geophys. Res. Lett.*, *32*, L08703, doi:10.1029/2005GL022478.

Mantua, N. J., et al. (1997), A Pacific interdecadal climate oscillation with impacts on salmon production, *Bull. Am. Meteorol. Soc.*, *78*, 1069–1079.

McDonald, K. C., et al. (2004), Variability in springtime thaw in the terrestrial high latitudes: Monitoring a major control on the biospheric assimilation of atmospheric CO_2 with spaceborne microwave remote sensing, *Earth Interact.*, *8*, 1–22.

Minobe, S. (2000), Spatio-temporal structure of the pentadecadal variability over the North Pacific, *Prog. Oceanogr.*, *47*, 382–408.

Running, S. W., et al. (2000), Global terrestrial gross and net primary productivity from the Earth Observing System, in *Methods in Ecosystem Science*, edited by O. Sala, R. Jackson, and H. Mooney, pp. 44–57, Springer, New York.

Running, S. W., et al. (2004), A continuous satellite-derived measure of global terrestrial primary productivity: Future science and applications, *Bioscience*, *56*, 547–560.

Schindler, D. W., and W. F. Donahue (2006), An impending water crisis in Canada's western prairie provinces, *Proc. Natl. Acad. Sci. U. S. A.*, *103*, 7210–7216.

Siedler, G., J. Church, and J. Gould (2001), *Ocean Circulation and Climate: Observing and Modelling the Global Ocean*, Academic, London.

Thompson, D. W. J., and J. M. Wallace (1998), The Arctic Oscillation signature in the wintertime geopotential height and temperature fields, *Geophys. Res. Lett.*, *25*, 1297–1300.

Trenberth, K. E., et al. (2007), Observations: Atmospheric surface and climate change, in *Climate Change 2007: The Physical Science Basis*, edited by S. Solomon et al., pp. 235–336, Cambridge Univ. Press, New York.

Wallace, J. M., and D. W. J. Thompson (2002), Annular modes and climate prediction, *Phys. Today*, *55*, 28–33.

Zhang, K., J. S. Kimball, M. Zhao, W. C. Oechel, J. Cassano, and S. W. Running (2007), Sensitivity of pan-Arctic terrestrial net primary productivity simulations to daily surface meteorology from NCEP-NCAR and ERA-40 reanalyses, *J. Geophys. Res.*, *112*, G01011, doi:10.1029/2006JG000249.

J. J. Cassano, Cooperative Institute for Research in Environmental Sciences and Department of Atmospheric and Oceanic Sciences, University of Colorado, Boulder, CO 80309-0216, USA.

J. S. Kimball and K. Zhang, Flathead Lake Biological Station, University of Montana, 32125 Bio Station Lane, Polson, MT 59860-9659, USA. (zhang@ntsg.umt.edu)

K. C. McDonald, Jet Propulsion Laboratory, California Institute of Technology, Mail Stop 300-233, 4800 Oak Grove Drive, Pasadena, CA 91101, USA.

S. W. Running, Numerical Terradynamic Simulation Group, University of Montana, 32 Campus Drive #1224, Missoula, MT 59812-1224, USA.